論文 95-9-9-16

Performance Improvement of a SCM Optical Coherent Detection System Using TCM Scheme

Hae Geun Kim* Regular Members

TCM 스킴을 이용한 일관성 광 검출 SCM 시스템의 전송 성능 개선

正會員 金 海 根*

ABSTRACT

Performance analysis of a subcarrier modulated (SCM) optical coherent detection (OCD) system has been carried out where quadrature phase-shift keying (QPSK) scheme and Trellis-Coded Modulation (TCM) scheme are used. Here, Frequency modulation (FM) is used as the principal modulation for the SCM system, while phase modulation (PM) has usually been employed. In order to increase throughput ratio or to permit normal operation at lower SNRs, TCM scheme could be applied to the specific communication systems containing non-linear devices, optical fiber link, satellite channel, etc.. But it is not easy to define the transmission quality of the system.

In this paper, the performance of the FM SCM system using TCM scheme is theoretically analyzed by defining the error bounds, an upper bound and a lower bound of error probability. Here, the noise variance at the FM discriminator output for each subcarrier has been calculated by programming numerical integration. The program is based on the mathematical formula used in describing an FM discriminator. Paralleling to this, computer simulations using communication software have been performed for both systems and then the results have been compared with the theoretical performance. Consequently, the system using TCM scheme obtains the coding gain of 3 dB over the SCM system using QPSK scheme.

要 約

QPSK와 TCM스킴을 이용한 일관성 광 검출 SCM 시스템에 대한 전송 성능을 분석 하였다. SCM 시스템에서는 주변조 스킴으로써 위상 변조 (PM)를 사용 하였으나 본 고에서는 주파수 변조 방식 (FM)을 이용하였다. 위성 통신 채널이나 광 링크 등 과 같이 비선형 소자를 포함하는 통신 시스템에서는, TCM기술이 전송부의 정보 처리율을 높이거나

*한국전자통신연구소(ETRI)
신호 서비스 연구실(ATM Signalling Service Section)
論文番號 : 95149-0415
接受日字 : 1995年 4月 15日

낮은 SNR에서도 정상적인 동작을 할 수 있게 하기 위한 수단으로서 사용 되어 왔다. 그러나 이러한 시스템들에 대한 전송 품질 을 정의 하기 위해서는 대단히 복잡한 과정을 거쳐야 한다.

본 논문에서는 수치 해석 법을 이용하여 각각의 부 반송파 별로 FM 변별기 출력 단의 잡음을 계산하여 SNR을 정의 하였다. 이어 주어진 SNR을 이용하여 TCM기술을 사용한 FM SCM 광 통신 시스템의 비트 에러 확률 (상한 및 하한 구간)들을 이론적으로 정의하여 비 코딩(QPSK)의 경우와 비교 하였다. 이와 동시에, 통신용 소프트웨어 패키지를 사용하여 TCM 또는 QPSK스킴을 결합한FM SCM시스템에 대한 시뮬레이션을 수행 하여 이론 치와 비교 검토 하였다. 그 결과 4-state 8-PSK TCM스킴을 이용하여 FM SCM 광 통신 시스템의 성능을 QPSK(비 코딩)을 사용 했을 경우에 비해 3dB의 전송 이득을 보았다.

Ⅰ. Introduction

Several approaches to optical multiplexing have been introduced[1]-[3]. Analog Subcarrier Multiplexing (SCM) is an attractive choice for the optical transmission of multigigabit/second signals, since it does not need electronics dealing with very high data rate[2]. SCM accommodates both the analog and the digital signal. By dint of subcarrier multiplexing techniques, multichannel transmission can be performed with one optical carrier. On the other hand, multiple optical carriers are required for Frequency Division Multiplexing (FDM) so that the speed of the photodetector will limit the maximum intermediate frequency (IF)[19]. Wavelength Division Multiplexing (WDM) is a second choice for coping with electronic data limitation for the optical baseband transmission. WDM can be used for both the analog and the digital signal. WDM and SCM can be implemented simultaneously for efficient utilization of the full optical bandwidth. Additionally, the coherent SCM system improved a 14dB in receiver sensitivity compared to a SCM direct detection system[22]. Therefore SCM and coherent detection are an interesting combination to provide high performance multichannel transmission

The SCM system employing the QPSK scheme permits multiplexing of several bit streams totaling to an overall data rate of 8 - 10 Gbit/s[4]. Here, if we employ the 8-state TCM instead of the QPSK, which occupies the same bandwidth as the QPSK, the performance can be improved because of the coding gain. While phase modulation (PM) has been mostly used as a principal modulation scheme, in this paper, FM is used for the SCM system. FM can be more interesting approach to optical fiber communication system, since a variation of input current to a semiconductor laser causes the frequency modulation of an optical output signal.

In addition to this, the phase noise of semiconductor laser is a major problem in coherent optical fiber communications, since it broadens the laser linewidth and deteriorates the performance. In recent study, Wu and Wang showed that an effect of phase noise is reduced by using a coding scheme[5]. Here, they employ the binary phase-shift-keying (BPSK) scheme with the heterodyne demodulation in conjunction with convolutional codes. The receiver sensitivity is improved by more than 9 dB due to the error correcting capability of the coding scheme. Also, Benedetto proposed by using the TCM scheme, the performance of the coherent optical channel employing a polarization shift keying

(POLSK) modulator[6] is improved by 3-4 dB without sacrificing bandwidth.

Error-control coding offers error-correcting capability by making the system tolerable against noise. Yet, this scheme needs several extra bits, so that a larger bandwidth is required. Therefore, the TCM scheme can be an attractive approach for improving receiver sensitivity and performance of an optical channel.

TCM has been developed actively since the publication by Ungerboeck[7] as a combined coding with modulation technique for digital transmission[8]-[11]. The main advantage of the TCM is the significant coding gain achieved over conventional uncoded multilevel modulation(eg., MPSK, MQAM, etc.) on the severely bandlimited additive white Gaussian noise channel, while maintaining the same data rate and transmitted power.

In view of modulation scheme aspects, if a digital communication system generates two information bits every T seconds, we can use one of two possible schemes: the QPSK scheme without coding and the 8-phase-shift keying (8-PSK) with a rate R = 2/3 convolutional coding.

The 8-PSK scheme utilizes the same bandwidth as that of the 4-PSK scheme. But a higher-order signal constellation system operates at a higher error rate at the same signal to noise ratio because of signal spacing in the constellation. Hence, the coding gain should overcome this penalty. In the TCM demodulator, the received signal is processed by demodulation and decoding in a single step. The Viterbi algorithm is used in decoding transmitted data.

In section Ⅱ, the concept of a heterodyne detection system and the noise characteristics of an FM detector are described. Computer simulation has been performed and analyzed in section Ⅲ. Finally conclusions and discussions are contained in section Ⅳ.

Ⅱ. System Description

The SCM system shown in Fig. 1 consists of an optical transmitter, a coherent heterodyne detection optical link, and a microwave receiver. The transmitter includes N channel SCMs, whose outputs are fed into an FM modulator.

At the optical receiver, the frequency modulated optical carrier is combined with the local laser signal by an optical coupler. A photodetector produces the microwave signal from the combined optical signal. The microwave signal consists of N channel SCM signals and the optical intermediate frequency (IF) signal between transmitted and local lasers. FM demodulator extracts the original SCM data from the amplified microwave signal.

2.1 Detection of an Optical SCM Signal

If an M- PSK signal has phase shift m and a symbol interval T, N channel SCM signal can be expressed as

$$X_N(t) = A_{sc}\sum_{i=1}^{N}\cos\{\omega_{sc_i}t + \phi_{m_i}(t)\} \qquad (1)$$

where

A_{sc} = Amplitude of subcarrier

$\phi_m = (2m+1)\frac{\pi}{M}$ = *angle of MPSK*

ω_{sc} = Subcarrier frequency

m = 0, 1, . , M-1

where subcarrier frequencis should be several times faster than the data rate. In an FM modulator, $X_N(t)$ is impressed on the frequency of an optical source. Hence, the outgoing optical signal from an FM subcarrier modula-

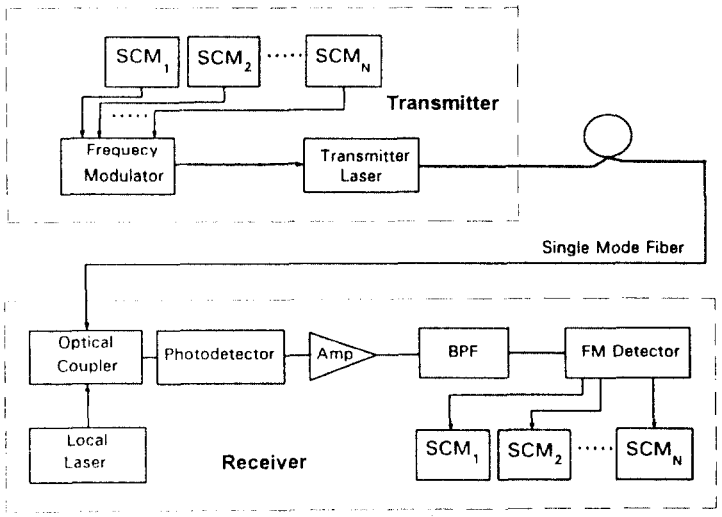

Figure 1. Block Diagram of N channel Subcarrier Modulated Coherent Optical Communication System.

tor is

$$i_{FM}(t)=\sqrt{P_s}\cos\left\{\omega_s t+\omega_d\int_{-\infty}^{t}\sum_{i=1}^{N}A_{sc_i}\cos[\omega_{sc_i}\tau+\phi_{m_i}(t)]\,d\tau\right\} \quad (2)$$

where

P_s = Peak power of transmitter laser

ω_s = Angular frequency of transmitter laser

ω_d = Radian value of frequency deviation of FM modulator.

Because $\omega_s \gg \omega_{sc}$, low-frequency(ω_{sc}) signals can directly FM modulate a laser diode for transmission along fiber. Here, modulating current should be small(a few mA) to minimize the undesired intensity modulation of a laser diode. So certain electronic followed by a laser diode is required to reduce the effect of the amplitude variation[19].

Let a local oscillator signal in the optical receiver in Fig. 1 be

$$i_{LO}=\sqrt{P_{LO}}\cos\omega_{LO}t \quad (3)$$

where P_{LO} is a peak power of a local oscillator and ω_{LO} is an angular frequency of a local oscillator. After an optical coupler combines a local laser signal with the incoming optical signal in (2), the output current of photodetector can be written as

$$i(t)=R[P_{LO}+P_S+2\sqrt{P_{LO}P_s}\cos\{\omega_{IF}t+\Phi(t)\}]+n(t) \quad (4)$$

$$\Phi(t)=\omega_d\sum_{i=1}^{N}\int_{-\infty}^{t}\cos\{\omega_{sc_i}t+\phi_{m_i}(t)\}\,dt$$

where R: responsivity of the photodetector

ω_{IF} : intermediate frequency

$\phi_m(t)$: composite microwave MPSK signal

$n(t)$: noise

The photodetector output $i(t)$ is passed through an amplifier which is tuned to $\omega_{IF}=\omega_s-\omega_{LO}$. Since the microwave frequency circuit

blocks the DC terms, the output electric signal $v(t)$ can be written as

$$v(t) = 2R\sqrt{P_{LO}P_S}\cos\{\omega_{IF} + \Phi(t)\} + n(t) \quad (5)$$

If we expand the information carrying portion of the photodetector output in the series of Bessel functions, we have

$$\begin{aligned} v(t) = 2R\sqrt{P_{LO}P_S} \sum_{n_1=-\infty}^{+\infty} \sum_{n_2=-\infty}^{+\infty} \cdots \sum_{n_N=-\infty}^{+\infty} J_{n_1}(\beta_1) \\ J_{n_2}(\beta_2)\cdots J_{n_N}(\beta_N) \cdot \cos\Big\{\omega_{IF}t + n_1\Big[\omega_{sc_1}t \\ + \phi_{m_1}(t)\Big] + n_2\Big[\omega_{sc_2}t + \phi_{m_2}(t)\Big] + \cdots \\ + n_N\Big[\omega_{sc_N}t + \phi_{m_N}(t)\Big]\Big\} \end{aligned} \quad (6)$$

where

$$\beta_i = \frac{\omega_d}{\omega_{sc_i}}: \text{ modulation index} \quad (7)$$

and $J_n(\beta)$ denotes an nth-order Bessel function. The desired signal component for each of the SCM signals is contained in the product of the first-order Bessel function. The other signal components contribute to the harmonic distortion and the intermodulation in the adjacent signal channels. The amplitude of the spectral line at the frequency $f_{IF} \pm nf_{sc}$ is given by $J_n(\beta)$.

2.2 Demodulation of an FM Signal

In an FM demodulation system shown in Fig. 2, any amplitude variation of the carrier is caused by noise alone, because a baseband signal modulates only the frequency of the FM carrier. The IF filter whose bandwidth can be $B = 2f_{sc}+2f_d$[12], where fsc is the subcarrier frequency and f_d is the frequency deviation, passes the signal with distortion and noise inside the bandwidth B.

A limiter suppresses such amplitude noise by waveshaping circuits whose outputs are nearly independent of modest changes in the carrier. The bandpass filter following the limiter removes the harmonics and selects the fundamental frequency component of $v_L(t)$.

The frequency-to-amplitude conversion is made in a discriminator with an envelope detector which extracts the envelope component of the signal. The baseband filter eliminates the DC component, so that the output signal becomes

$$v_B(t) = \frac{A_L\omega_d}{2\pi}\sum_{i=1}^{N}\cos\Big[\omega_{sc_i}t + \phi_{m_i}(t)\Big] \quad (8)$$

where A_L is the output amplitude of a limiter. Therefore, when we compare the detected signal in (8) with the modulating signal in (1), the two signals are identical except the amplitude determined by the FM demodulator. A delay-and-multiply discriminator is popularly used for the optical fiber communication system because implementation is easier.

2.3 Noise Characteristics of an FM Demodulator

In a typical coherent detection system, we can assum that shot noise generated by a local laser overwhelms the thermal noise generated in the postoptical-detection portion of the receiver. And the shot noise can be mod-

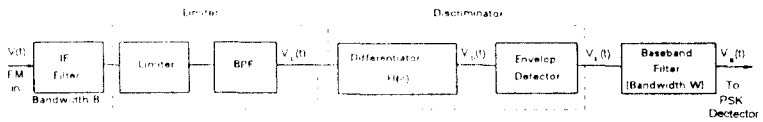

Figure 2. Block Diagram of an FM Demodulator.

eled as white Gaussin noise. Hence, the output noise of the IF filter can be written in the narrowband representation, which has the Rayleigh-distributed envelope and an uniformly distributed phase. In order to calculate the output noise of an FM discriminator, we set the modulating signal $\phi(t)=0$ in (5), because the noise is almost independent of the signal.

If the signal-to-noise ratio (SNR) is large (usually most of the time), $|n_c(t)| \ll A_L$ and $n_s(t) \ll A_L$, where n_c and n_s are the quadrature components of the noise. After the output noise of the limiter passes through a discriminator with an envelope detector, the noise can be written as

$$v_B(t)=\frac{A_L}{2\pi A_{IF}}\frac{d}{dt}n_s(t) \tag{9}$$

where A_{IF} is the output amplitude of a IF filter. The power spectral density of $n_s(t)$ is η over $|f| \le B/2$, and the transfer function of the differentiator is presented in an imaginary form as $j\omega/2\pi$. Hence, the noise spectrum of the differentiator output can be

$$S_n(\omega)=\left[\frac{A_L\omega}{2\pi A_{IF}}\right]^2\eta \tag{10}$$

for $|f| \le B/2$ and zero otherwise. Equation (10) represent the non-linear characteristic of an FM detection because the noise power is a fuction of squared frequency. The spectrum of this colored-noise at the discriminator output is illustrated in Fig. 3. The discriminating action proffers the parabolic shape of the noise spectrum which affects the performance of the FM system in the presence of noise.

Let the baseband filter have the bandwidth W which should be less than B. The output noise power is

$$N_0=\frac{2}{3}\frac{A_L^2\eta}{A_{IF}^2}W^3 \tag{11}$$

2.4 Evaluation of Noise

A PSK detector is used in extracting the source data from the baseband filter output signal. If the SCM signal with noise is passed through an integration-and-dump (I&D) circuit, the output becomes

$$Z(t)=\frac{A_L\omega_d}{2\pi}\int_0^T\cos\omega_{sc}t\cos\left[\omega_{sc}t+\phi_m(t)\right]dt + \int_0^T n(t)\cos\omega_{sc}t\,dt \tag{12}$$

where T is a symbol interval and $(\omega_{sc}T)/2\pi$ is a constant. Since $n(t)$ is a Gaussian noise, the second term of (12) is also a Gaussian.

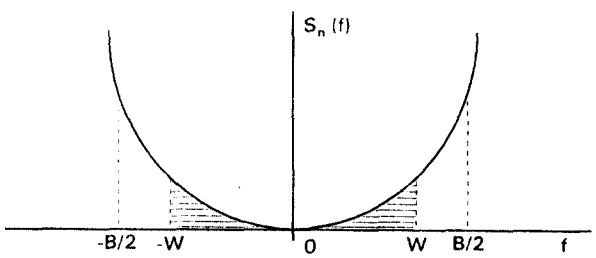

Figure 3. The Power Spectrum of FM Discriminator Output.

But, an FM discriminator modifies the noise spectrum, so that the resulting noise is colored, which has zero-mean with non-uniform spectral density. Since $E[N_C] = 0$ and $E[N_C^2] = \sigma^2 = Var[N_C]$, we have

$$E\{N_c^2\} = E\left\{\int_0^T\int_0^T n(t)n(t')\cos(\omega_{sc}t)\cos(\omega_{sc}t')\,dt\,dt'\right\} = E\left\{\int_0^T\int_0^T R_n(t-t')\cos(\omega_{sc}t)\cos(\omega_{sc}t')\,dt\,dt'\right\} \quad (13)$$

In order to calculate the autocorrelation of the discriminator output noise, it is necessary to transform (10) into the time domain. Thus we get

$$R_n(\tau) = \frac{1}{2\pi}\int_{-\infty}^{\infty} S(\omega)\, e^{j\omega\tau} d\omega \quad (14)$$

Since $n(t)$ is real and even, we can write

$$R_n(\tau) = \frac{A_n}{\pi}\int_0^{\infty} \omega^2 \cos\omega\tau\, d\omega \quad (15)$$

where

$$A_n = \left(\frac{A_L}{2\pi A_W}\right)^2 \eta \quad (16)$$

which is the amplitude of noise. After the signal is passed through the baseband filter with the cut-off frequency W, by substituting the $R_n(t-t')$ of (15) into (13), we obtain the unnormalized noise variance in terms of $(t-t')$, which can be written as

$$E\{N_c^2\} = E\left\{\int_0^T\int_0^T\left[\frac{2A_n}{\pi}\cos W(t-t') - \frac{4A_n}{\pi(t-t')^3}\sin W(t-t') + \frac{2A_nW^2}{4\pi(t-t')^2}\sin W(t-t')\right]\cdot\cos(\omega_{sc}t)\cos(\omega_{sc}t')\,dt\,dt'\right\} \quad (17)$$

In the next section, we have evaluated $E[N_c^2]$ in (17) with the known parameters, T and ω_{sc}, by computer programming which is written in C language. Numerical calculation is used in estimating the noise power.

Ⅲ. COMPUTER SIMULATION

In this section, for the theoretical analysis, the variance of noise at an FM discriminator and the baseband filter output is estimated by programming with C language. Then the calculated performance curves, which are based on the results, are plotted in terms of the SNR. We have also simulated the subcarrier modulated optical coherent communication system using the QPSK scheme and the TCM scheme. The simulations have been performed using COMDISCO SPW software package[13]. Then the results are compared with the calculated performance in the computer simulation section.

Also the main purpose of the simulations in this section is to compare the SCM system using the QPSK scheme with the system using the TCM scheme. Because of that, one subcarrier modulated channel is handled in the SCM systems.

3.1 Estimation of the Noise Variance and the Calculated Performance

In order to estimate the noise variance which is expressed in double-integral form, we have used numerical integration for the programming. Set $x_0 = a$, $h = (b-a)/M$, $y_0 = c$, $k = (d-c)/N$, and $f_{ij} = f(y_i, y_{j+1})$. Then we can

generalize the following formulas which combine the rectangular rule with trapezoidal rule as[14]

$$\int_a^b \int_b^d f(x,y)\,dx\,dy = \frac{hk}{4}\sum_{i=0}^{m}\sum_{j=0}^{n}\left(f_{i-1,j-1}+f_{i-1,j}+f_{i,j-1}+f_{ij}\right) = hk\cdot\sum_{i=0}^{m}\sum_{j=0}^{n} w_{ij} f_{ij} \quad (18)$$

where

w_{ij} = 1 for the interior grid points.

w_{ij} = 0.25 for the four corner points.

w_{ij} = 0.5 for the rest of boundary points.

For theoretical analysis of the system performance, the variance of noise at FM discriminator output expressed in (17) is estimated by means of a computer program.

The programs are run for the given parameters: the symbol interval T is 20 ns, the subcarrier frequencies ω_{sc} are 0.1, 0.15, and 0.2 GHz; the bandwidth of baseband filter, W, is 0.5 GHz. These parameters are described in the next section (also see Table 1.). The results of computer derived variances are 9.527, 18.294, and 29.589 nW/Hz for f_{sc} = 0.1, f_{sc} = 0.15, and f_{sc} = 0.2 GHz, respectively.

In order to determine the SNR based on the calculated noise variance, the average energy of the two binary digits at the integration-and-dump (I&D) output is computed as

$$\overline{E_b} = \frac{A^2T}{2} + \frac{(-A^2)T}{2} = A^2T$$

where A is the amplitude of the carrier. When we let A be unity, we can derive the output SNR expressed as T/σ^2 where T is 20 ns and σ^2 is the calculated noise variance for the bandwidth of baseband filter, W = 0.5 GHz.

The TCM scheme used in the simulation is shown in Fig. 4(a). A rate 1/2 convolutional encoder with a 8-PSK mapper is contained, where two shift registers (L=2: the constraint length) and two modulo-2 adders are used. In accordance with normal operation, the shift registers are assumed to be cleared (zero), when the first message bit arrives. Hence, we can construct the trellis diagram as shown in Fig. 4(b)where the solid line denotes the output sequence which is generated by the '0' input bit. And a dotted line denotes the output sequence which is generated by the '1' input bit.

In order to plot the calculated performance curve, we substitute the calculated SNR into the formula, which expresses the bit error probability for each system. For a 4-state 8-

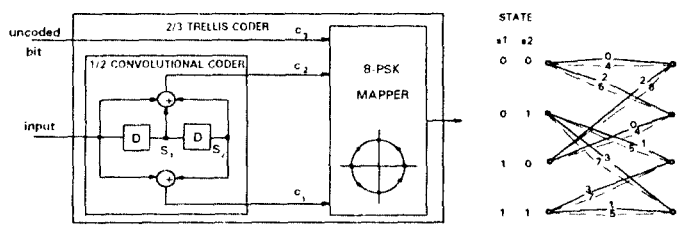

Figure 4. (a) 4-state 8-PSK TCM Scheme, and (b) its Trellis Diagram.

PSK TCM system, the following equation is used in determining the upper bound of error probability as[4]

$$P_b \le \frac{1}{2}Q\left(\sqrt{4E_b/N_0}\right) + \frac{1}{2}D^{d_c^2}Q\left(\sqrt{d_c^2 E_b/N_0}\right)\left.\frac{\partial T(D,I)}{\partial I}\right|_{I=1,D=e^{-E_b/4N_0}} \quad (19)$$

where $d_c^2 = 4.586$ which denotes the minimum distance associated with the error event, $\partial T(D,I)/\partial I$ represents the weaker transfer function bound, and Q(.) describes the Gaussian error integral as

$$Q(x) = \frac{1}{\sqrt{2\pi}}\int_x^\infty \exp\left(\frac{y^2}{2}\right)dy$$

The first term in the right-hand side of (19) can be the lower bound of error probability of a 4-state 8-PSK TCM scheme. The bit error probability of the QPSK scheme is provided by $Q(\sqrt{2E_b/N_0})$. We have plotted the calculated performance curves for the uncoded QPSK scheme and a 4-state 8-PSK TCM scheme which includes the upper bound and lower bound of error probability in Fig. 8-10.

3.2 Computer Modeling and Simulation of the SCM system

A block diagram of the communication system that we simulated is shown in Fig. 5. It should be noted that the simulation configuration does not include optical signals, and that only the DSP equivalents of RF and microwave frequencies are used. The basic time unit represented 1 ns so that a frequency of 40 Hz represented 40 GHz. Similarly, the subscriber frequencies of 100, 150, and 200 MHz were scaled to 0.1, 0.15, 0.2 Hz, respectively. These frequencies are harmonics of 1/T, and thus are orthogonal to each other over a common T-second pulse interval. And the period T = 20 ns is equivalent to 5 x 10^7 symbols/s.

There is 50 MHz space between the IF frequency and the data frequency for the first subcarrier. So extremely narrow laser linewidth is required for this system. The parameters used in the simulation are written in Table 1.

In Fig. 5, the outputs of QPSK modulators are summed and FM-modulated for transmission, where a subcarrier is modulated. In the

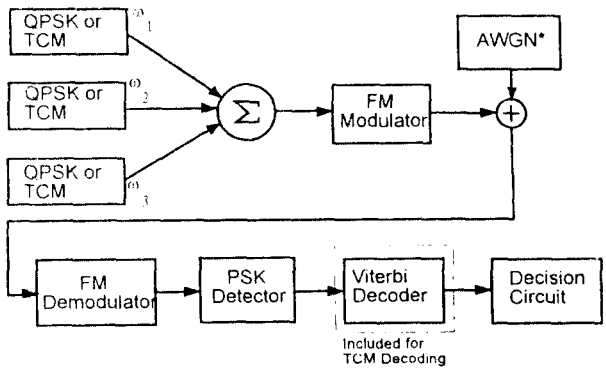

Figure 5. Block Diagram of the Simulation System.

Table 1. Parameters for the Simulation

Parameter	Specification
Sampling Frequency	400[GHz]
Symbol Duration	20[ns]
Subcarrier Frequency	0.1, 0.15, and 0.2 [GHz]
Maimum Freq. Deviation	1[GHz]
f_{IF}	40[GHz]

channel, the Gaussian noise is added and then the noisy SCM signal is fed into an FM demodulator where the baseband signal and the noise with a quadratic spectrum are detected. . In the PSK detector in Fig. 6, the signal is multiplied by the subcarrier and then the resulting signal is passed through an integration-and-dump circuit which extracts the source data.

The sampled signal of the PSK detector output is compared with the source data by the decision circuit. Here, the source data is transmitted through a delay device from the source. When the simulation run is completed, the results, which include the total number of output samples, errors, and the BER are stored in the SPW file.

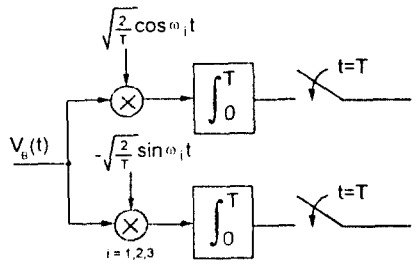

Figure 6. Schematic Diagram of a PSK Detector Used in the simulation Model.

For synchronization, we have used a locally generated clock which has approximately the same timing as that of the incoming carrier signal. Delay elements are used in adjusting the time difference between the source data and the delayed (or distorted) output data.

The SCM system which employs a 4-state 8-PSK TCM system, as shown in Fig. 5, contains a TCM encoder and a TCM decoder. A TCM encoder is designed as shown in Fig. 4. A TCM decoder employing the Viterbi algorithm regenerates the source data from the 8-PSK input signal. The detected signal is handled the same manner as that of QPSK.

3.3 Simulation Results and Performance Evaluation

From the simulation results, the noise signal at a discriminator output is drawn in a frequency domain by SPW as shown in Fig. 7. When we compare this figure to Fig. 3 which is based on the theory, both curves are almost identical each other.

The sampling rate f_s is one of the principal parameters of the simulation because it should be a sufficient number of samples in a period of the highest frequency in the system (f_{IF} = 40 GHz). The choice of f_s = 480 GHz

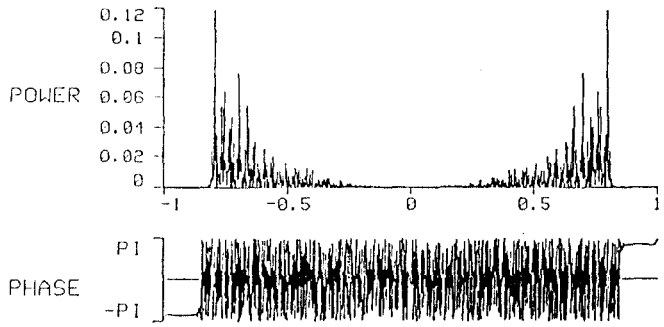

Figure 7. The Simulated Noise of the Discriminator Output.

resulted in 12 samples per period at fIF. So typical running times were on the order of 11 hours for 10 million samples Running time of each simulation is approximately 110 hours for 10^9 samples. Since the Monte Carlo simulation method[16] is used in estimating the performance, we can estimate the BER up to 10^{-5}.

In order to calculate the SNR from the simulation result, let the receiver input amplitude be unity. In the simulation model for the SCM system, the input SNR in terms of simulation parameters is described as[15]

$$SNR_{input} = \frac{f_s}{4\sigma^2 B_{in}} \quad (20)$$

where f_s = sampling frequency.

σ^2 = variance of noise.

B_{in} = the bandwidth of the IF filter at the front end of the receiver.

The simulation results for each subcarrier frequency are shown in Table 2. In this table, we have listed the BER's for the given noise variance. The BER vs the SNR graphs for each subcarrier is plotted as shown in Fig. 8-10. Here, the 'O' and '△' marked curves denote the simulation results for a 4-state 8-PSK TCM scheme and a QPSK scheme respectively.

According to the results, TCM scheme achieves 3 dB coding gain compared to QPSK over the SCM optical channel using the same bandwidth. The SCM systems using higher frequencies receive more noise power over the colored Gaussian noise channel. So the system using fsc= 0.1 GHz offers 3 dB higher quality than that of the system using f_{sc}= 0.15 GHz does. Similarly, the system using f_{sc}= 0.15 GHz has 3 dB advantage in performance compare to the system using f_{sc}= 0.2 GHz.

We have also found that both the upper and the lower bound of error probability curves for TCM scheme are overlapped in the

Table 2. Simulation Results of the SCM Systems.

AWGN	f_{sc}=0.1 GHz		f_{sc}=0.15 GHz		f_{sc}=0.2 GHz	
	TCM	QPSK	TCM	QPSK	TCM	QPSK
12.0	4.0×10^{-3}	NC	NC	NC	NC	NC
9.5	7.9×10^{-4}	8.0×10^{-3}	NC	NC	NC	NC
9.0	5.6×10^{-4}	6.3×10^{-3}	NC	NC	NC	NC
7.5	1.1×10^{-4}	2.7×10^{-3}	3.2×10^{-3}	NC	NC	NC
6.75	4.2×10^{-5}	1.6×10^{-3}	6.3×10^{-4}	NC	NC	NC
6.0	NC	7.9×10^{-4}	NC	6.3×10^{-3}	NC	NC
5.25	NC	NC	1.6×10^{-4}	3.2×10^{-3}	NC	NC
4.75	NC	1.7×10^{-4}	6.3×10^{-5}	2.5×10^{-3}	2.5×10^{-3}	NC
4.5	NC	NC	2.8×10^{-5}	1.9×10^{-3}	NC	NC
3.75	NC	3.4×10^{-5}	NC	6.8×10^{-4}	5.6×10^{-4}	7.2×10^{-3}
3.0	NC	NC	NC	1.4×10^{-4}	7.9×10^{-5}	2.5×10^{-3}
2.75	NC	NC	NC	NC	2.0×10^{-5}	1.4×10^{-3}
2.5	NC	NC	NC	2.2×10^{-5}	4.0×10^{-6}	7.9×10^{-4}
2.0	NC	NC	NC	NC	NC	1.6×10^{-4}
1.5	NC	NC	NC	NC	NC	2.5×10^{-5}

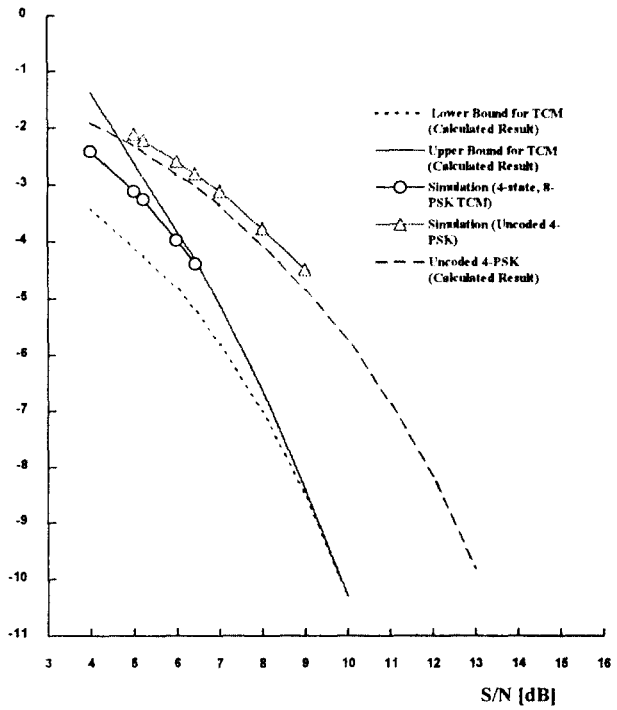

Figure 8. Error Probability of the SCM Systems Using a 4-State 8-PSK TCM Scheme and a QPSK Scheme (f_{sc} = 0.1 GHz).

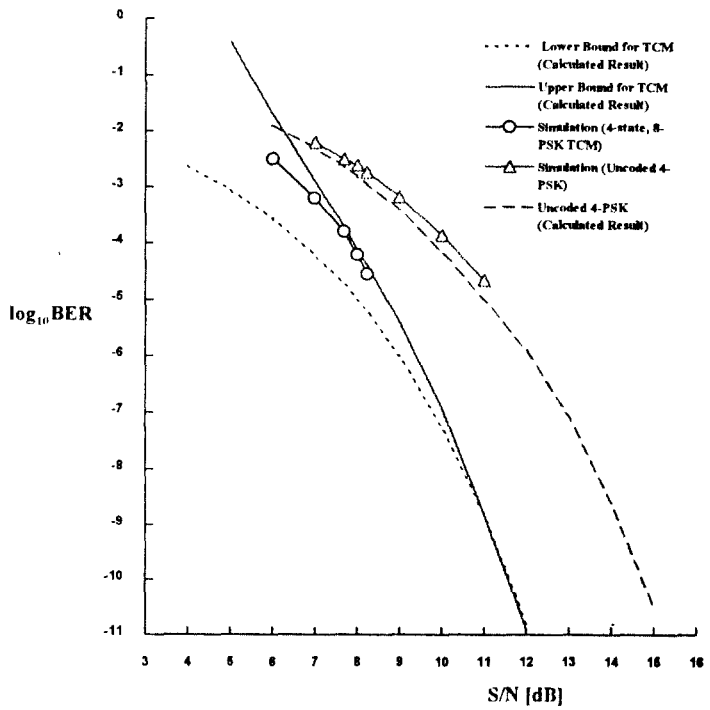

Figure 9. Error Probability of the SCM Systems Using a 4-State 8-PSK TCM Scheme and a QPSK Scheme (f_{sc} = 0.15 GHz).

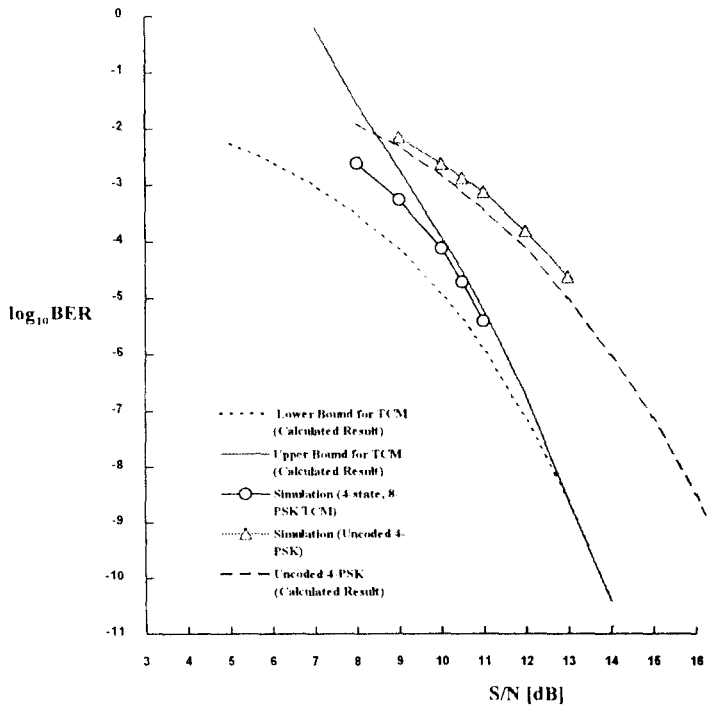

Figure 10. Error Probability of the SCM Systems Using a 4-State 8-PSK TCM Scheme and a QPSK Scheme (f_{sc} = 0.2 GHz).

range of BER $< 10^{-9}$. So the both error probability bounds at ultra-low BERs are almost same.

Ⅳ. Conclusion

In this paper, we have investigated the possible advantages of the subcarrier modulated optical coherent communication system using the TCM scheme over the QPSK scheme. From the simulation results, the SCM system using the 4-state 8-PSK TCM scheme provides a 3 dB gain over the SCM system using the uncoded QPSK scheme.

We have found that a TCM scheme can be applied to optical fiber channels as a performance improving technique.

In order to analyze the SCM system theoretically, the calculated variance of an FM discriminator output is used in determining the SNR of the SCM system. We have defined the performance in terms of the SNR, the upper bound and the lower bound of error probability, of the SCM system using a TCM scheme. We have realized that both bounds are superposed when the BER $< 10^{-9}$. Also, the lower bound of error probability can be expressed by a much simpler equation than that of the upper bound of error probability. Therefore, by using the lower bound of error probability alone, we can completely estimate the performance range BER$<10^{-9}$.

The system performance could be improved by employing a higher state TCM, by using Table II in [9], 8-state 8-PSK TCM gaining 3.6 dB , 16-state 8-PSK TCM gaining 4.13

dB, etc.. Multidimensional TCM (constant amplitude type) can also be used in improving the system which contains non-linear devices.

REFERENCES

1. R. Olshansky and R. Gross, "Subcarrier Multiplexed Coherent Lightwave Systems for Video Distribution," *IEEE Jour. on Selected Areas in Comm.*, vol. 8, N0. 7, Sep. 1990.
2. P. Hill and R. Olshansky, "Bandwidth Efficient Transmission of 4 Gb/3 on Two Microwave QPSK Subcarriers Over a 48 km Optical Link," *IEEE Photonic Tech. Letters*, vol. 2, No. 7, July. 1990.
3. P. Hill and R. Olshansky, "Multigigabit Subcarrier Multiplexed Coherent Lightwave System," *IEEE Jour. of Lightwave Tech.*, Vol. LT-10, No. 11, Nov. 1992.
4. R. Olshansky and R. Gross, "Multichannel Coherent FSK experiments Using Subcarrier Multiplexing Techniques," *IEEE Jour. of Lightwave Tech.*, vol. 8, N0. 3, Aug. 1990.
5. J. Wu, C. Wang, and I. Wu, "Coding to Relax Laser Linewidth Requirement and Improve Receiver Sensitivity for Coherent Optical BPSK Communications," *IEEE J. Lightwave Technol.*, Vol. 8, No. 4, April. 1990.
6. S. Benedetto, A. Milanesi, G. Olmo, and P. Poggiolini, "Applications of Trellis Coding to Coherent Optical Communications Employing Polarization Shift Keying Modulation," *Electronic Letters*, Vol. 27, June. 1991.
7. G. Ungerboeck, "Channel Coding with Multilevel/Phase Signal," *IEEE Trans. Information Theory*, vol. IT-28, No. 1, January. 1982.
8. G. Ungerboeck, "Trellis-Coded Modulation with Redundant Signal Sets Part I: Introduction," *IEEE Comm. Mag.*, February. 1987.
9. G. Ungerboeck, "Trellis-Coded Modulation with Redundant Signal Sets Part Ⅱ: Introduction," *IEEE Comm. Mag.*, February. 1987.
10. E. Biglieri and P. J. Mclane, "Uniform Distance and Error Probability Properties of TCM Schemes," *IEEE Trans. Commun.*, Vol. 39, January. 1991.
11. Ross McKay, P. J. Mclane and E. Biglieri, "Error Bound for Trellis-Coded MPSK on a Fading Mobile Satellite Channel," *IEEE Trans. Commun.*, Vol. 39, December. 1991.
12. A. Bruce Carlson, *Communication Systems*, Third Edition, McGraw-Hill, New York, 1986.
13. Comdisco Operating Manual, *Signal Processing Worksystem and SPW*(TM), Comdisco Systems, Inc., 1991.
14. J. F. Hart, *Computer Approximations*, John Wiley & Sons, New York, 1968.
15. Gerard Lachs, S. Zaidi, and A. Singh, "Sensitivity Enhancement Using Coherent Hetrodyne Detection," *IEEE Jour. Lightwave Tech.*, Vol. 12, No.6, June. 1994.
16. M. C. Jeruchim, "Techniques for Estimating the Bit Error Rate in the Simulation of Digital Communication Systems," *IEEE Journal on Selected areas in Commu.*, vol. SAC-2, No.1, Jan. 1984.
17. D. Duff, "Computer-Aided Design of Digital Lightwave Systems," *IEEE Journal on Selected areas in Commu.*, vol. SAC-2, No.1, Jan. 1984.
18. Allen Cherin, *An Introduction to Optical Fibers*, McGraw-Hill, Inc., 1983.
19. Joseph C. *Palais, Fiber Optic Communications*, p.223, Prentice-Hall, Inc., 1984
20. S. Burington, *Handbook of Mathematical Tables and Formulas*, Handbook Publishers, Sandusky, Ohio, 1953.
21. A. Papoulis, Probability, *Random Variables, and Stochastic Process*, Second Edition, McGraw-Hill, New York, 1984.
22. R. Gross and R. Olshansky, "Third-Order

Intermodulation Distortion in Coherent Subcarrier-Multiplexed System," *IEEE Photonic Tech. Letters*, vol. 1, No. 4, April. 1989.

金 海 根(Hae Geun Kim) 정회원

1977년 2월 : 경북대학교 전자공학과 졸업
1994년 8월 : 미국 University of South Florida 전기공학과 졸업(공학박사)
1980년 8월~현재 : 한국전자통신연구소 재직, 교환연구단 신호서비스연구실 책임연구원
※주관심 분야 : modulation, trellis coding, optical fiber communications, mobile communications